EXPERIMENTAL AND NUMERICAL ANALYSIS OF A HYBRID-VENTILATED ROOM

F.CRON[(1)], M. EL MANKIBI[(2)], C.INARD[(1)], P.MICHEL[(2)]
1 : LEPTAB, University of La Rochelle, Avenue Michel Crépeau, F-17042 La Rochelle Cedex 01
Phone :+33.(0)5.46.45.86.24., Fax : +33.(0)5.46.45.82.41, fcron@univ-lr.fr, cinard@univ-lr.fr
2 : LASH, ENTPE, Rue Maurice Audin, F-69518 Vaulx-en-Velin
Phone :+33.(0)4.72.04.70.31., Fax : +33.(0)4.72.04.70.41, elmankibi@entpe.fr, pierre.michel@entpe.fr

Summary
This study, carried out within the frame of the IEA Annex 35 " Hybrid Ventilation in New and Retrofitted Buildings", was undertaken to model a hybrid-ventilated room, and to implement control strategies.
An experimental cell, called HYBCELL, was designed at the ENTPE-LASH Laboratory to provide both mechanical and natural ventilation. Various sensors were installed in the cell for the indoor environment, in the hall, and outside for the boundary conditions.
Modeling was performed by ENTPE-LASH and LEPTAB. The collaboration, supported by the ADEME (Agence De l'Environnement et de la Maîtrise de l'Energie), resulted in models that describe the cell, its mass and thermal transfers to make a comparative study between several ventilation systems and controls.

Introduction

The purpose of a hybrid ventilation system is to use both natural and mechanical driving forces to provide a good and healthy indoor environment at the lowest cost. Although there were projects on natural ventilation like AIOLOS (Allard, 1998) or NatVent (NatVent, 1999), there remains a lack of knowledge concerning the implementation of hybrid ventilation systems, the use of such technologies and their suitable control strategies. For these reasons, the IEA decided to develop the Annex 35 "Hybrid Ventilation in New and Retrofitted buildings" (Annex 35, 2000). This study is part of this Annex and consists in applying control strategies to hybrid ventilation systems in office buildings or schools. Both experimental and modeling approaches were used for this purpose.

Description of the experimental room

Location and architecture of HYBCELL
The ENTPE-LASH experimental room is located in Lyon (France) and is on the first level of a two-storey building. The only external wall is a Northern-Eastern facade that makes a 70° angle with the horizontal plane. The cell is surrounded by a heated cell and hall.
The cell was retrofitted to be comparable to an office, so a false ceiling and a access floor were installed to reduce the height. HYBCELL is 2.95 m high, 3.5 m wide and 5.1 m long.
There are six windows placed symmetrically on the facade as illustrated on figure 1.

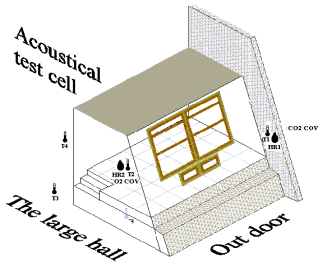

Figure 1: Architecture of HYBCELL

Material used for HYBCELL
The external wall has a light thermal capacity: it consists of two layers of wood filled with some polystyrene. The partitions are made of two thin steel layers filled with rock wool. The floor is a wooden one and some plaster board with rock wool composes the ceiling. So the global thermal capacity of HYBCELL is quite light.
The windows are double pane ones. The shade on the facade (windows and wall) was calculated to estimate the incident direct and diffuse radiation loads.

Experimental devices
The room has been equipped with air temperature, dry bulb temperature and CO_2 sensors to collect information on indoor air quality and comfort parameters. Parameters like wind speed, wind direction, and diffuse and direct solar radiation were required too. The ENTPE meteorological station provided us with these boundary conditions. The windows were equipped with a driving system, composed by step by step motors. This device can control window openings accurately and automatically,

and can switch from the natural ventilation mode to the mechanical one.
A circular duct network with variable power exhaust fan was installed at the top of the cell. The heating device was a 3 [kW] radiant panel with a proportional controller and the occupancy was simulated by CO_2 generation and heat supply devices.

Models used for the simulations
We used the object oriented solver SPARK to compute the entire problem with differential and non linear equations. All the equations had to be implemented in SPARK, so the model used ones based in part of a previous study done for the IEA Annex 35 (Cron et al, 2002).

Models describing the air within the zone
A single zone model with an assumed hydrostatic pressure variation was considered. We wrote the "pure" air mass balance and the pollutant mass balance equations. For a zone "i" with n openings:

$$\sum_{j=1}^{n} m_{asji} - \sum_{j=1}^{n} m_{asij} = 0 \text{ and}$$

$$\sum_{j=1}^{n} m_{esji} - \sum_{j=1}^{n} m_{esij} + S_{es} = V \frac{d\rho_{es}}{dt}$$

m_{asji} [kg_{as}/s] is the pure air mass flow rate from the zone j to the zone i, and likewise for the CO_2 mass flow rate m_{esij} [kg_{es}/s]. S_{es} is the pollutant source [kg_{es}/s] and V the volume [m^3]. The thermal balance is:

$$\sum_{j=1}^{n} \left(m_{asji} cp_{as} + m_{esji} cp_{es}\right) T_j - \sum_{j=1}^{n} \left(m_{asij} cp_{as} + m_{esij} cp_{es}\right) T$$
$$+ S_{es} cp_{es} \left(T_{es} - T\right) + P_{conv} + P_{loadconv} + \Phi_{conv}$$
$$= \left(\rho_{as} cp_{as} + \rho_{es} cp_{es}\right) V \frac{dT}{dt} + cp_{es} V T \frac{d\rho_{es}}{dt}$$

For closure, ideal gas law was used:

$$P = \left(\rho_{as} r_{as} + \rho_{es} r_{es}\right)\left(T + 273.15\right) \qquad [Pa]$$

Air flow rates through upper and lower windows and that due to infiltration were computed using a power law relation:

$$Q = C \cdot \left(\Delta P\right)^n = C \cdot \left(P_i - P_j\right)^n . \qquad [m^3.s^{-1}]$$

C and n were obtained experimentally for infiltration (El Mankibi et al, 2001):

$$Q = 0.00617 \cdot \left(\Delta P\right)^{0.7293} \qquad [m^3.s^{-1}]$$

For the narrow windows n = 0.5.
To obtain the mass air flow rate, thermal buoyancy difference was accounted using a correction coefficient K_Q (Feustel et al, 1990):

$$m_{asji} = \rho_{ij} K_Q Q = \rho_{ij} K_Q C\left(P_i - P_j\right)^n \qquad [kg.s^{-1}]$$

where $\rho_{ij} = \frac{\rho_i + \rho_j}{2}$.

The air flow through the large central windows was estimated using the De Gidds and Phaff method (De Gidds et al, 1982):

$$Q = \frac{A}{2} \sqrt{C_1 U_{met}^2 + C_2 H \Delta T + C_3} \qquad [m^3.s^{-1}]$$

with C_1 = 0.001, C_2 = 0.0035 and C_3 = 0.01, U_{met} is the wind velocity in [$m.s^{-1}$].

We wrote a model that computes the total pressure loss in a ventilation system with a volumetric air flow rate Q. The pressure losses include the friction losses ΔP_{lin} and those due to duct fittings ΔP_{sing}. If the flow is laminar, the friction coefficient is given by 64/Re, if the flow is turbulent, the Colebrook's implicit equation was used. The dynamic loss coefficient values were taken from litterature (Feustel et al, 1990). The fan was modeled in the usual way using a fan performance curve.

Description of the room envelope
The conductive heat transfer was described by an electrical 2R-3C model to have a good response to an indoor high frequency excitation (Rumianowsky, 1989).

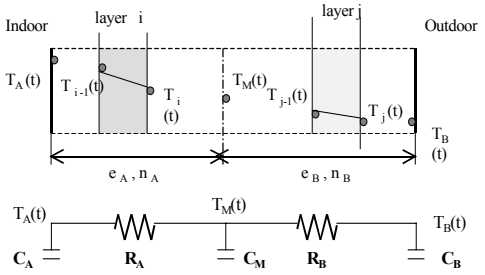

Figure 2: Description of the electrical model

We made a comparison between the response of this model and the one given by a finite difference model. The position of the intermediate node was set to the optimum value of e_A that provided the minimum error E_{eA}.
E_{eA} is given by:

$$E_{eA} = \int_0^{\infty} \left| T_{A\,finite\,difference} - T_A \right| dt$$

If T_e is the outdoor temperature, T_v the sky temperature and β the angle between the surface and the horizontal plane (β = 70°), the

outdoor long-wave radiation is given by:

$$\Phi_{netGLOe} = \varepsilon_e \sigma_o S_e \left(\frac{(1-\cos(\beta))}{2} \left(T_e^4 - T_{se}^4 \right) \right) + \varepsilon_e \sigma_o S_e \left(\frac{(1+\cos(\beta))}{2} \left(T_v^4 - T_{se}^4 \right) \right) \quad [W]$$

Here temperatures are in [K].
The solar radiation absorbed by the external wall surface was calculated given the incident solar radiation and the surface solar properties.

The convective heat transfer at the outdoor surface was given by:

$$\Phi_{conve} = h_{conve} S (T_e - T_{se}) \quad [W]$$

T_{se} is the surface temperature and $h_{conve} = c + dU_{met}^{\ n}$ where c = 2.5, d = 3.5, n = 1 according to (Ferries, 1980).

Indoors, the long-wave radiative heat transfer model was a mean radiative temperature model which took into account the radiative part of the internal loads and of the heating system. For the surface i:

$$\Phi_{netGLOi} = h_{rmi} S_i (T_{rm} - T_{si}) \quad [W] \quad \text{with:}$$

$$h_{rmi} = 4\sigma_o \varepsilon_i \left(\frac{T_{si} + T_{rm}}{2} + 273.15 \right)^3 \quad [W.m^{-2}.K^{-1}]$$

$$\text{and } T_{rm} = \frac{\sum_{i=1}^{n} (h_{rmi} S_i T_{si}) + P_{rad} + \Phi_{rad}}{\sum_{i=1}^{n} h_{rmi} S_i} \quad [K]$$

The short-wave radiation transmitted indoors was assumed to be distributed to the illuminated fraction of each surface. One part was absorbed, the other reflected in a diffuse way. The global diffuse radiation was distributed over the surface depending on their area ratio and then absorbed (for the windows, one fraction is retransmitted outdoors).

Convection indoors was obtained by:

$$\Phi_{convi} = h_{convi} S (T - T_{si}) \quad [W]$$

$$\text{where } h_{convi} = a |T - T_{si}|^b \quad [W.m^{-2}.K^{-1}]$$

the values of a and b were taken from (Allard, 1987) depending on the configurations.

Simulations

Simulations were performed after having adjusted the thermal models to experiments. Two periods were simulated: 3 weeks in winter and 3 weeks in spring (the first is still during the heating period). Heating hours were from 7h00 to 18h00, Monday to Friday, with a set point temperature of 20 [°C]. That for non-heating hours was 18 [°C]. The ventilation hours are from 8h00 to 18h00, Monday to Friday. Two persons were assumed to occupy the cell 36 h a week. The internal loads (lighting, PC) were set to 165 [W]. Two simulations of mechanical ventilation system were performed: the first one without any window opening (mode 1), whereas for the second (mode 2) the large window was opened when the indoor and outdoor air temperatures were higher than 23 [°C] and 12 [°C] respectively. A natural ventilation system was simulated too (mode 3) with a constant opening of the inlets (the narrow windows) during the ventilation hours. Like the mode 2, this control strategy allowed some window airing. For the first three modes, control was on indoor air temperature only. A fourth simulation was run and concerned a hybrid ventilation system (mode 4). The control was on indoor temperature for heating and window airing, and on CO_2 for the inlet openings. When CO_2 concentration was higher than 1200 [ppm], the fan switched on to ensure the minimum required flow rates. The dead band value was 100 [ppm]. The performances of each system are presented in terms of air temperature, CO_2 concentration, time length of exposure to a poor indoor air quality (CO_2>1000 [ppm]) and energy efficiency (fan and heating system).

Results and discussion

In winter, the modes 1 and 2 were the same, since the windows were closed. Natural ventilation gave lower exposure time length (figure 3) and lower mean CO_2 concentration (figure 4) but the driving forces increased the air flow rates (figure 5) and thus the heating consumption: 8% more compared to the modes 1 and 2.

Mode	Exposure in winter	Exposure in spring
Mechanical 1	7h/36h of work	20.3h/36h of work
Mechanical 2	7h/36h of work	10h/36h of work
Natural	2.3h/36h of work	6.7h/36h of work
Hybrid	6h/36h of work	7.7h/36h of work

Figure 3: Exposure time length to CO_2 concentration higher than 1000 [ppm]

With hybrid ventilation, when there were fewer people in the room, the CO_2 decreased and the inlets got closed, so there was no waste of energy during non-occupancy. The maximum

and mean values of CO_2 were higher with hybrid ventilation because of the CO_2 control strategy dead bands that imposed the fan to switch on at 1200 [ppm]. But hybrid ventilation provided a shorter exposure to high CO_2 concentration and 6.8% of energy savings with the fan off and with fewer heating needs due to lower global air flow rates (figures 4 and 5).

Winter	Max T	Mean T	Max CO2	Mean CO2	Fan	Heating
	[°C]	[°C]	[ppm]	[ppm]	[kWh]	[kWh]
Mechanical 1	21.15	20.13	1056.2	819.3	1.0E-03	219.9
Mechanical 2	21.15	20.13	1056.2	819.3	1.0E-03	219.9
Natural	21.2	20.1	1067	759.8	0.0E+00	237.3
Hybrid	21.16	20.15	1079.1	840.8	0.0E+00	205
Spring	**Max T**	**Mean T**	**Max CO2**	**Mean CO2**	**Fan**	**Heating**
	[°C]	[°C]	[ppm]	[ppm]	[kWh]	[kWh]
Mechanical 1	28	21.8	1126	960.8	1.1E-03	12.73
Mechanical 2	27.4	21.4	1105.7	833.2	1.1E-03	13.14
Natural	27.4	21.3	1394.1	840.1	0.0E+00	13.3
Hybrid	27.5	21.5	1201	895.5	3.9E-05	12.32

Figure 4: Results of simulations

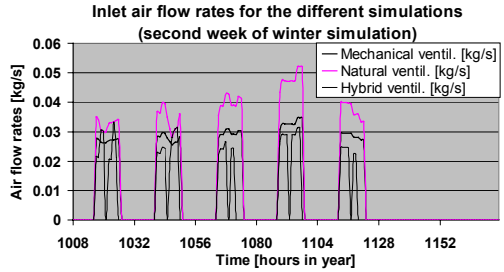

Figure 5: Ventilation air flow rates in winter

In spring, since the facade was facing North, there was no direct solar radiation in the afternoons. Indoor temperature was mainly dependent on the internal loads and ventilation. Window airing had no much influence on indoor air temperature (the outdoor temperature wasn't much lower than that indoors), but had a greater influence on high CO_2 concentration exposure (figures 3 and 4). Natural ventilation was too unreliable: some mornings, when the driving forces were too low and the windows closed, low air change rate occurred and led up to 1394 [ppm] of CO_2. With hybrid ventilation, even if the mean value of CO_2 was higher, the high CO_2 concentration exposure was lower than those with modes 1 and 2 (figures 3 and 4). Energy consumption for hybrid ventilation is the lowest one for both seasons. High CO_2 concentration exposure with hybrid ventilation was between natural ventilation and mechanical ventilation ones for both seasons and was much lower than that for mode 1 in spring.

Conclusion

For both simulated seasons, hybrid ventilation showed better performances in terms of temperatures, CO_2 concentration exposure and energy consumption than traditional ventilation systems. It can be a good solution for indoor air quality at lower costs, but it requires control strategy on both temperature and CO_2. Some more case studies need to be performed, with another exposition to the sun and with a higher thermal capacity (possibilities of night cooling).

References

Allard, F. (1987). *Contribution à l'étude des transferts de chaleur dans les cavités thermiquement entraînées à grand nombre de Rayleigh*, Thèse d'Etat, INSA de Lyon, 1987.

Allard, F., Ed (1998). *Natural Ventilation in Buildings : A Design Handbook*, James & James, London, UK, 1998.

Annex 35 (2000). CD with *State of the art of Hybrid Ventilation*, IEA ECBCS Annex 35 HybVent, 2000.

Cron, F. and Inard, C. (2002). Hybrid Ventilation Simulation of Control Strategies – WG A1 input to first parameter study simulation in WG B7, Technical report F7-081, IEA Annex 35, 2000.

De Gidds, W. and Phaff, H. (1982). "Ventilation Rates and Energy Consumption due to Open Windows", *Air Infiltration Review*, Vol.4, No 1, pp 4-5, 1982.

El Mankibi, M., Michel, P. and Guarracino, G. (2001). "Control Strategies for hybrid ventilation development of an experimental device", *Proceedings of the 22nd Annual AIVC Conference*, Bath, UK, 11-14 September 2001.

Ferries, B. (1980). *Contribution à l'étude des enveloppes climatiques et aide à leur conception par micro-ordinateur*, Thèse Doct.-Ing., INSA de Lyon, 1984.

Feustel, H.E. and Rayner-Hooson, A., Ed (1990). COMIS fundamentals, Technical report LBNL-28560, Lawrence Berkeley National Laboratory, 1990.

NatVent (1999). *Natural Ventilation for Offices*, The EU NatVent Consortium, BRE, Watford, UK, 1999.

Rumianowski, P., Brau, J. and Roux, J.J. (1989)."An adapted model for simulation of the interaction between a wall and the building heating system", *Thermal performance of the exterior envelopes of buildings IV Conference*, Orlando, USA.